J|A|C|S ARTICLES

Published on Web 08/03/2010

^{129}Xe NMR Study of the Framework Flexibility of the Porous Hybrid MIL-53(Al)

Marie-Anne Springuel-Huet,*,† Andrei Nossov,† Ziad Adem,† Flavien Guenneau,† Christophe Volkringer,‡ Thierry Loiseau,‡ Gérard Férey,‡ and Antoine Gédéon†

Laboratoire de Chimie de la Matière Condensée, UMR CNRS 7574, Université Pierre et Marie Curie, Univ. Paris 06, F 75252 Paris Cedex 05, France, and Institut Lavoisier, UMR CNRS 8180, Université de Versailles Saint Quentin, 45, avenue des Etats-Unis, 78035 Versailles Cedex, France

Received April 19, 2010; E-mail: marie-anne.springuel-huet@upmc.fr

Abstract: The metal−organic framework MIL-53 exhibits a structural transition between two possible porous structures, so-called large-pore (*lp*) and narrow-pore (*np*) forms, depending on the temperature or when guest molecules are adsorbed. ^{129}Xe NMR has been used to study the *lp* → *np* transition induced by the adsorption of xenon as revealed by the adsorption isotherms. The NMR spectra show that the two structures, characterized by two distinct lines, coexist for xenon pressures above 5×10^4 Pa at room temperature, but a complete transformation is achieved when the temperature is decreased. An original interpretation of the NMR results allowed us to quantify the rate of the structural transformation. In particular, at room temperature, we have shown that 28% of the channels remain open. Two possible interpretations of the hysteresis observed in the chemical shift variation versus xenon pressure are proposed.

1. Introduction

Porous materials find many industrial applications in various fields such as catalysis including enantioselective catalysis, gas separation, gas storage, drugs delivery, electronics, sensors, etc. Recently, the interest in these solids has shifted from inorganic zeolites to new materials,[1−3] particularly to the new class of porous hybrid solids (see ref 4 and references therein), featuring association in the same framework of inorganic and organic moieties (polycarboxylates, polyphosphonates) linked exclusively by strong bonds. They combine the robustness of zeolites and the versatility of carbon chemistry, which enables tuning of the pore size and the existence of very high specific areas, reaching sometimes several thousands of square meters per gram. Moreover, although they are often rigid, some hybrid frameworks can be highly flexible (see ref 5 and references therein), allowing sometimes a change of the cell volume by more than 300%.[6] This feature has been mainly studied and explained by Férey and Kitagawa groups.[5,7]

In this domain, the contribution from Férey's group focuses on one part of a series of materials, named MIL-*n* (MIL standing for Materials of Institut Lavoisier). They exist with numerous cations, currently from mono- to tetravalent, and present various pore structures (channels or cages) and pore sizes. When trivalent metals (Al, Ga, Cr, Fe, In, etc.) are concerned, the MIL-53 structure represents an aristotype of flexible topologies.[8−15] In this structure, organic ligands link infinite chains of $MO_4(OH)_2$ octahedra, trans-connected via μ_2-hydroxo groups. The assembly forms one-dimensional channels running parallel to the chains (Figure 1).

Upon the action of an external stimulus, it is a bistable system, and its contraction/expansion depends on the presence of guest molecules. It may vary from a lozenge shape, 2.6×13.6 Å^2, (in the narrow-pore (*np*) form), for instance when water is adsorbed), to an almost square shape, 8.6×8.6 Å^2 (in the large-pore (*lp*) form, when the tunnels are either empty or completely filled).[8−21] The pore dimensions are tightly correlated to the nature, the size, and the amount of guest molecules (H_2O, N_2,

† Université Pierre et Marie Curie.
‡ Université de Versailles Saint Quentin.

(1) Fan, J.; Slebodnick, C.; Angel, R.; Hanson, B. E. *Inorg. Chem.* **2005**, *44*, 552.
(2) Zhang, Y.; Saha, M. K.; Bernal, I. *Cryst. Eng. Commun.* **2003**, *5*, 34.
(3) Loiseau, T.; Férey, G. *J. Fluorine Chem.* **2007**, *128*, 413.
(4) Férey, G. *Chem. Soc. Rev.* **2008**, *37*, 191.
(5) Férey, G.; Serre, C. *Chem. Soc. Rev.* **2008**, *38*, 1380.
(6) Serre, C.; Mellot-Draznieks, C.; Surblé, S.; Audebrand, N.; Filinchuk, Y.; Férey, G. *Science* **2007**, *124*, 13519.
(7) Kitagawa, S.; Uemura, K. *Chem. Soc. Rev.* **2005**, *34*, 109.
(8) Barthelet, K.; Marrot, J.; Riou, D.; Férey, G. *Angew. Chem., Int. Ed.* **2002**, *41−2*, 281.
(9) Serre, C.; Millange, F.; Thouvenot, C.; Noguès, M.; Marsolier, G.; Louër, D.; Férey, G. *J. Am. Chem. Soc.* **2002**, *124*, 13519.
(10) Loiseau, T.; Serre, C.; Huguenard, C.; Fink, G.; Taulelle, F.; Henry, M.; Bataille, T.; Férey, G. *Chem.—Eur. J.* **2004**, *10*, 1373.
(11) Volkringer, C.; Loiseau, T.; Guillou, N.; Férey, G.; Elkaïm, E.; Vimont, A. *Dalton Trans.* **2009**, 2241.
(12) Vougo-Zanda, M.; Huang, J.; Anokhina, E.; Wang, X.; Jacobson, A. J. *Inorg. Chem.* **2008**, *47*, 11535.
(13) Chaplais, G.; Simon-Masseron, A.; Porcher, F.; Lecomte, C.; Bazer-Bachi, D.; Bats, N.; Patarin, J. *Phys. Chem. Chem. Phys.* **2009**, *11*, 5241.
(14) Anokhina, E.; Vougo-Zanda, M.; Wang, X.; Jacobson, A. J. *J. Am. Chem. Soc.* **2005**, *127*, 15000.
(15) Whitfield, T. R.; Wang, X.; Liu, L.; Jacobson, A. J. *Solid State Sci.* **2005**, 1096.
(16) Serre, C.; Bourrelly, S.; Vimont, A.; Ramsahye, N. A.; Maurin, G.; LLewellyn, P. L.; Daturi, M.; Filinchuk, Y.; Raynaud, O.; Barnes, P.; Férey, G. *Adv. Mater.* **2007**, *19*, 2246.
(17) Bourrelly, S.; Llewellyn, P. L.; Serre, C.; Millange, F.; Loiseau, T.; Férey, G. *J. Am. Chem. Soc.* **2005**, *127*, 13519.
(18) Millange, F.; Serre, C.; Guillou, N.; Férey, G.; Walton, R. *Angew. Chem., Int. Ed.* **2008**, *47*, 4100.

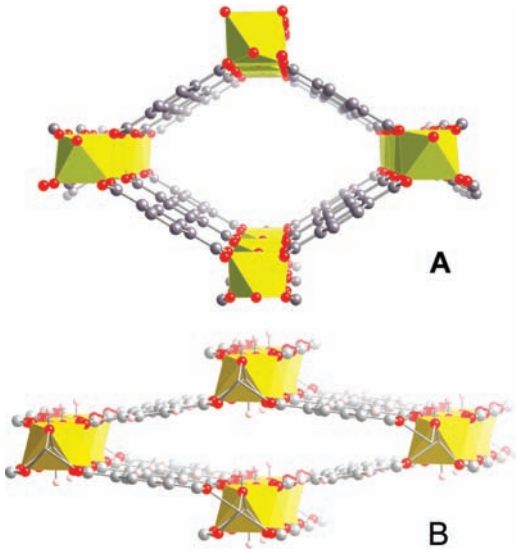

Figure 1. Large-pore (*lp*) forms of MIL-53 structure type (metal, yellow; O, red; C, gray; H, pink).

CO_2, hydrocarbons, pyridine, lutidine, methanol, etc.).[17−30] The structural transitions occur at different temperatures, depending on the nature of the metal and the extent of loading. They have recently been studied by molecular dynamics and density functional theory calculations.[25−30] The *np* → *lp* transition was studied by Brown et al.[31] as a function of temperature in the absence of any host−guest interaction. The transitions show very low kinetics. Surprisingly, the structural transition shows a large temperature hysteresis in the range of about 125−375 K that might be due to an energetic barrier between the two states, corresponding to the two structures. In the case of adsorbate-induced transition, Neimark et al. applied a stress-based model that successfully describes the hysteresis observed in the adsorption−desorption isotherms.[32]

^{129}Xe NMR of adsorbed xenon is a technique particularly suitable to investigate porous solids, such as zeolites, amorphous silica−alumina, polymers, carbons, peptides, etc.[33−42] Xenon is an inert gas and an ideal probe owing to its great sensitivity due the high polarizability of the atom. The chemical shift strongly depends on the interactions of the xenon atoms with their environment. In particular, the chemical shift depends on the nature (chemical composition, "rugosity") of the pore surface. In microporous solids, it increases with the Xe loading due to additional Xe−Xe interactions inside the pore, these interactions depending on the pore size and shape as well. Extensive work has been done on zeolite microporous solids and revealed a relationship between the chemical shift at zero coverage, i.e., in the absence of Xe−Xe interaction, and the pore size of the zeolite structures.[33] It has been reported that xenon is able to induce a phase transition of MIL-53(Al).[43] At 273 K and above, the adsorption−desorption isotherms have one step in the pressure range from 0 to 1.2×10^5 Pa, corresponding to the *lp* → *np* transition. At 220 K and below, there are two distinct steps, corresponding successively to the previous transition and then the reverse one (*np* → *lp*). This is in good agreement with the results obtained on CO_2 adsorption which showed that, for a sufficient pressure depending on the temperature, the pores are able to reopen to adsorb more guest molecules.[16]

In the case of flexible frameworks, the Xe atoms can reveal the pore changes that they induce themselves. We report here the structural changes of MIL-53 as a function of xenon pressure and temperature as observed by ^{129}Xe NMR.

2. Experimental Section

MIL-53(Al) Characterization. The aluminum-based MIL-53 was synthesized as described in previous literature.[20] The specific surface area, pore volume, and pore diameter were determined from N_2 adsorption data obtained at 77 K using an ASAP 2010 Micromeritics instrument. Prior to the analysis, the sample was outgassed at 423 K until a stable static vacuum of 0.25 Pa was reached. It should be noted that the N_2 adsorption−desorption isotherms (type I, not shown) are perfectly reversible without any hysteresis and follow the Langmuir equation. The Langmuir surface area of the sample studied is 1644 m^2/g, corresponding to a microporous pore volume of 0.60 cm^3/g. The pore size, determined by the Horwath−Kawazoe approach with cylinder pore geometry, averages 8.7 Å.

^{129}Xe NMR. Before NMR experiments, the MIL-53(Al) was evacuated under dynamic high vacuum ($<10^{-2}$ Pa) at 423 K overnight (heating rate 24 K/h).

(19) Llewellyn, P. L.; Maurin, G.; Devic, T.; Loera-Serna, S.; Rosenbach, N.; Serre, C.; Bourelly, S.; Horcajada, P.; Filinchuk, Y.; Férey, G. *J. Am. Chem. Soc.* **2008**, *130*, 12808.
(20) Trung, T. K.; Trens, P.; Tanchoux, N.; Bourelly, S.; Llewellyn, P. L.; Loera-Serna, S.; Serre, C.; Loiseau, T.; Fajula, F.; Férey, G. *J. Am. Chem. Soc.* **2008**, *130*, 16926.
(21) Millange, F.; Guillou, N.; Walton, R. I.; Grenèche, J.-M.; Margiolaki, I.; Férey, G. *Chem. Commun.* **2008**, 4732.
(22) Ramsahye, N. A.; Maurin, G.; Bourrelly, S.; Llewellyn, P. L.; Loiseau, T.; Férey, G. *Phys. Chem. Chem. Phys.* **2007**, *9*, 1059.
(23) Ramsahye, N. A.; Maurin, G.; Bourrelly, S.; Llewellyn, P. L.; Loiseau, T.; Serre, C.; Férey, G. *Chem. Commun.* **2007**, 3261.
(24) Ramsahye, N. A.; Maurin, G.; Bourrelly, S.; Llewellyn, P. L.; Devic, T.; Serre, C.; Loiseau, T.; Férey, G. *Adsorption* **2007**, *13*, 461.
(25) Ramsahye, N. A.; Maurin, G.; Bourrelly, S.; Llewellyn, P. L.; Devic, T.; Serre, C.; Loiseau, T.; Férey, G. *J. Phys. Chem. C* **2008**, *112*, 514.
(26) Salles, F.; Jobic, H.; Maurin, G.; Koza, M. M.; Llewellyn, P. L.; Devic, T.; Serre, C.; Férey, G. *Phys. Rev. Lett.* **2008**, *100*, 245501.
(27) Rosenbach, N.; Jobic, H.; Ghoufi, A.; Salles, F.; Maurin, G.; Férey, G. *Angew. Chem., Int. Ed.* **2008**, *47*, 6611.
(28) Salles, F.; Ghoufi, A.; Maurin, G.; Bell, R.; Mellot-Draznieks, C.; Férey, G. *Angew. Chem., Int. Ed.* **2008**, *47*, 8487.
(29) Coombes, D.; Corà, F.; Mellot-Draznieks, C.; Bell, R. *J. Phys. Chem. C* **2009**, *113*, 544.
(30) Coudert, F.-X.; Mellot-Draznieks, C.; Fuchs, A. H.; Boutin, A. *J. Am. Chem. Soc.* **2009**, *131*, 3442.
(31) Liu, Y.; Her, J.-H.; Dailly, A.; Ramirez-Cuesta, A. J.; Neumann, D. A.; Brown, C. M. *J. Am. Chem. Soc.* **2008**, *130*, 11813.
(32) Neimark, A. V.; Coudert, F.-X.; Boutin, A.; Fuchs, A. H. *J. Phys. Chem. Lett.* **2010**, *1*, 445.
(33) Bonardet, J.-L.; Fraissard, J.; Gedeon, A.; Springuel-Huet, M.-A. *Catal. Rev.—Sci. Eng.* **1999**, *41*, 115.
(34) Terskikh, V.; Mudrakovskii, I. L.; Mastikhin, V. M. *J. Chem. Soc., Faraday Trans.* **1993**, *8923*, 4239.
(35) Walton, J. H. *Polym. Polym. Composites* **1994**, *21*, 35.
(36) Mirabella, F. M., Jr.; McFaddin, D. C. *Polymer* **1996**, *376*, 931.
(37) Mansfeld, M.; Flohr, A.; Veeman, W. S. *Appl. Magn. Reson.* **1995**, *83−4*, 573.
(38) Simonutti, R.; Bracco, S.; Comotti, A.; Mauri, M.; Sozzani, P. *Chem. Mater.* **2006**, *1819*, 4651.
(39) Locci, E.; Roose, P.; Bartik, K.; Luhmer, M. *J. Colloid Interface Sci.* **2009**, *3302*, 344.
(40) Romanenko, K. V.; Fonseca, A.; Dumonteil, S.; Nagy, J. B.; d'Espinose de Lacaillerie, J.-B.; Lapina, O. B.; Fraissard, J. *Solid State Nucl. Magn. Reson.* **2005**, *282−4*, 135.
(41) Saito, K.; Kimura, A.; Fujiwara, H. *Magn. Reson. Imag.* **2003**, *313/4*, 401.
(42) Rubin, S. M.; Spence, M. M.; Pines, A.; Wemmer, D. E. *J. Magn. Reson.* **2001**, *1521*, 79.
(43) Boutin, A.; Springuel-Huet, M.-A.; Nossov, A.; Gédéon, A.; Loiseau, T.; Volkringer, C.; Férey, G.; Coudert, F.-X.; Fuchs, A. *Angew. Chem., Int. Ed.* **2009**, *48*, 1.

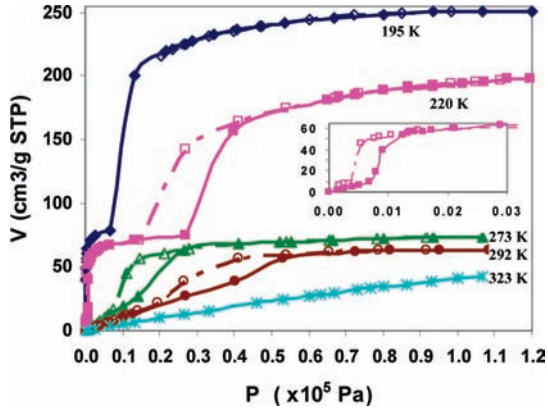

Figure 2. Xe adsorption (solid symbols) and desorption (open symbols) isotherms measured at 195 (lozenges), 220 (squares), 273 (triangles), 292 (circles), and 323 K (stars). Inset: Low-pressure region of the isotherm at 220 K.

For the thermally polarized ^{129}Xe experiments, xenon was adsorbed at room temperature using a homemade apparatus. For equilibrium pressures >1.5 $\times$ 10^5 Pa, the desired amount of gas was trapped in the sample tube using liquid nitrogen. The system was allowed to equilibrate overnight.

Variable-pressure ^{129}Xe NMR spectra were recorded at 295 K using thermally polarized xenon with a Bruker AMX 300 spectrometer operating at 83.02 MHz. A 90° pulse (ca. 17 μs) was used. Typically 10^3-10^5 scans, with a repetition time up to 20 s, were recorded. The T_1 relaxation time of the different signals (adsorbed Xe) was measured to be between 4 and 5 s.

At low Xe loading (1.33 kPa), variable-temperature experiments were performed using laser-polarized xenon under continuous gas flow using a home-built system on the same spectrometer between 373 and 183 K. Typically 512 scans, with a repetition time of 1 s, were recorded. At high Xe loading (9.6 $\times$ 10^4 Pa), thermally polarized xenon was used, and typically up to 2 $\times$ 10^4 scans were recorded between 343 and 233 K. The spectra were recorded every 2 K after the sample was allowed to equilibrate for a few minutes.

The chemical shifts are referenced to gaseous xenon extrapolated to zero pressure (0 ppm).

The spectra were decomposed, and the chemical shift tensor components as well as the width and intensity of the lines were determined using DMFit software.[44]

3. Results

Xe Adsorption−Desorption Isotherms. Xe adsorption−desorption isotherms have been measured in the 0−1.2 $\times$ 10^5 Pa pressure range at different temperatures: 195, 220, 273, 292, and 323 K.[43] Below 300 K, the isotherms present one or two steps and hysteresis loops (Figure 2). At 323 K, the adsorption isotherm presents no step and can be described by the Langmuir equation on the whole set of data. The amount adsorbed at saturation depends on the channel form. For a given form, it increases when temperature decreases.

The isosteric heat of adsorption has been calculated at different regions of the isotherms using the Clausius−Clapeyron relation. It varies with the Xe concentration from 16−20 kJ/mol for the open *lp* form to ca. 30 kJ/mol for the closed *np* form of the channels (Figure S1, Supporting Information).

Variable-Pressure Experiments. The variable-pressure experiments performed with hyperpolarized ^{129}Xe were conducted from low to high Xe pressures, in the range of about 1.33 $\times$ $10^3-1.33$ $\times$ 10^5 Pa, at 295 K. We also performed NMR experiments using thermally polarized ^{129}Xe, which allowed us to record spectra while decreasing the pressure.

Figure 3 shows the NMR spectra of xenon recorded at adsorption (A) and desorption (B). At low pressure, a single isotropic line is observed (line *a*). As the pressure increases, a broad asymmetric line appears at higher chemical shift (line *b*). Its intensity increases with xenon pressure at the expense of the isotropic line. MAS NMR experiments revealed that line *b* is anisotropic (Figure S2, Supporting Information). The isotropic chemical shift of line *b* was determined using DMFit software after deconvolution of the spectra when necessary.

The isotropic chemical shift of both lines increases with the xenon pressure. The chemical shift variations of both lines, *a* and *b*, and the line width variation of line *a* are given in Figure 4. Above P(Xe) $\approx$ 2.67 $\times$ 10^4 Pa, the chemical shift variation of line *a* exhibits a large hysteresis loop. In contrast, there is no hysteresis for line *b*. However, during desorption, this line disappears at P(Xe) = 2.67 $\times$ 10^4 Pa, whereas it appeared at 5.33 $\times$ 10^4 Pa during adsorption.

During adsorption, the width of line *a* drastically increases when line *b* appears; during desorption, it returns to its initial value when line *b* disappears, showing a large hysteresis in the same pressure range as for the chemical shift variations (Figure 4).

As pressure increases, the intensity of line *b* increases at the expense of line *a* up to $P \approx 1.33 \times 10^5$ Pa. In order to check the impact of high pressure, thermally polarized Xe spectra have been recorded at higher Xe pressure (ca. 3 $\times$ 10^5 Pa), obtained by trapping a known amount of Xe gas in the sample tube using liquid nitrogen. The intensity of line *a* increases again (see spectrum in Figure S3, Supporting Information).

The variation of the chemical shift tensor components of line *b* is given in Figure 5. With increasing xenon pressure, one component (δ_{11}) has nearly the same magnitude, while the two others (δ_{22} and δ_{33}) are slightly deshielded. δ_{11} has been attributed to the direction of the channel axis, whereas δ_{22} and δ_{33} have been attributed to the minor and major axes of the elliptical cross section of the channels, respectively (vide infra).

Variable-Temperature Experiments. The spectra were recorded every 2 K at decreasing and increasing temperatures, but only typical spectra recorded when temperature was decreasing are displayed in Figures 6 and 9. The single isotropic line *a*, observed at low pressure, moves downfield when temperature decreases. At 222 K, a broad anisotropic line appears as the isotropic line begins to broaden and finally disappears at 218 K. The anisotropic line *b* also moves downfield and broadens when temperature decreases below 218 K (Figure 6) and finally disappears below 200 K.

The chemical shift and the line width variations of line *a* as a function of temperature are reported in Figure 7 for P(Xe) = 1.33 kPa. Above ca. 300 K, the chemical shift variation is linear, and the line width remains practically constant. Below that temperature, the slopes of both chemical shift and line width variations drastically increase as the temperature decreases, until line *a* disappears in favor of line *b*.

Above room temperature, the isotropic line shows a shoulder that increases with increasing temperature. This is characteristic of a partial exchange between adsorbed and interparticle gaseous Xe atoms at high temperature.

As in the variable-pressure experiments, the anisotropic line appears or disappears at a certain temperature, depending on

(44) Massiot, D.; Fayon, F.; Capron, M.; King, I.; Le Calvé, S.; Alonso, B.; Durand, J. O.; Bujoli, B.; Gan, Z.; Hoatson, G. *Magn. Reson. Chem.* **2002**, *40*, 70.

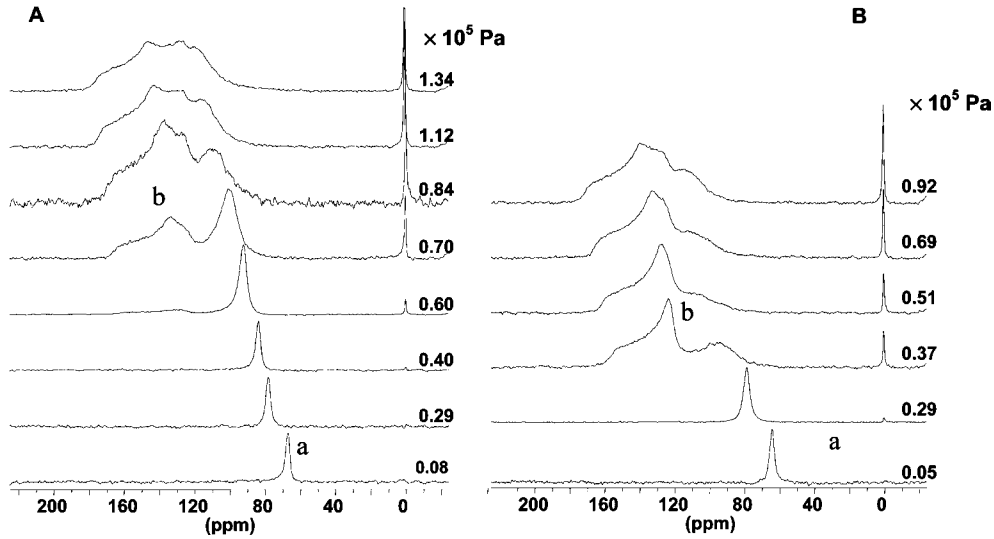

Figure 3. ^{129}Xe NMR spectra (thermally polarized ^{129}Xe) versus xenon pressure recorded at adsorption (A) and desorption (B).

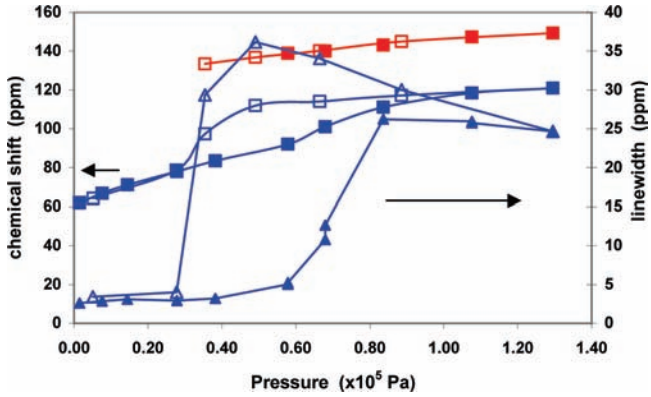

Figure 4. Chemical shift variation (squares) of line *a* (blue) and line *b* (red) and line width variation (triangles) of line *a* as a function of pressure. Adsorption, solid symbols; desorption, open symbols.

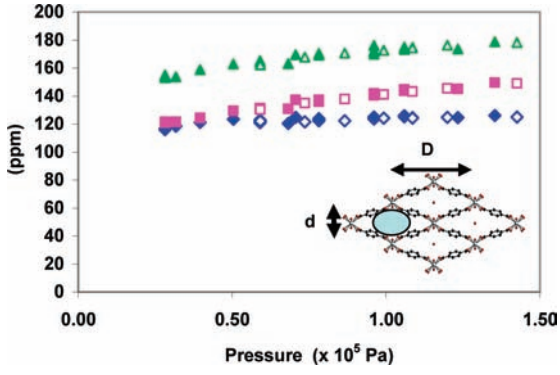

Figure 5. Chemical shift tensor components of line *b* versus xenon pressure: δ_{11} (blue lozenges) along the channel axis, δ_{22} (pink squares) along the minor axis (*d*) of the cross section, δ_{33} (green triangles) along the major axis (*D*) of the cross section. Solid symbols, thermally polarized ^{129}Xe; open symbols, optically polarized ^{129}Xe.

both the direction and the rate of the variation. We could observe line *b* up to 245 K when temperature was increasing. The chemical shift tensor of line *b* as a function of temperature is reported in Figure 8.

The experiments performed at high Xe pressure (9.6×10^4 Pa) are reported in Figure 9. The intensity of line *b* increases at the expense of line *a* as temperature decreases. At 333 K, the spectrum practically shows line *a* only. The chemical shifts of both lines *a* and *b* increase as temperature decreases.

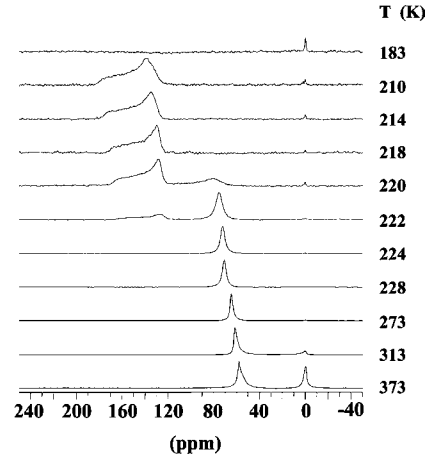

Figure 6. ^{129}Xe NMR spectra (hyperpolarized ^{129}Xe) versus temperature for $P = 1.33$ kPa (decreasing temperature).

4. Discussion

Xe Adsorption−Desorption Isotherms. The starting points of the isotherms ($P = 0$) versus temperature can be analyzed from the recent structural results reported by Brown,[31] extracted from neutron powder diffraction and inelastic neutron scattering. Once dehydrated, MIL-53(Al) exhibits the *lp* form.[10,31] After cooling at 77 K, the stable form corresponds to the *np* arrangement, and this explains the different behaviors of the isotherms observed when temperature varies.

At 323 K, the absence of any peculiarity on the isotherm curve in the pressure range from 0 to 1.1×10^4 Pa indicates that, during the entire process, Xe is adsorbed in the *lp* form. The situation begins to change at lower temperatures, with the appearance of a two-step behavior and an inflection zone that depends on the temperature of the measurement: 4×10^4−5.3×10^4 Pa at 292 K, 1.3×10^4−2.7×10^4 Pa at 273 K, and 7×10^2−1.2×10^3 Pa at 220 K (inset of Figure 2). Above these critical pressures, adsorption increases, associated with the *lp* → *np* transition, the narrow pores having a greater affinity for Xe atoms.[43] At larger pressures, the isotherms at 292 and 273

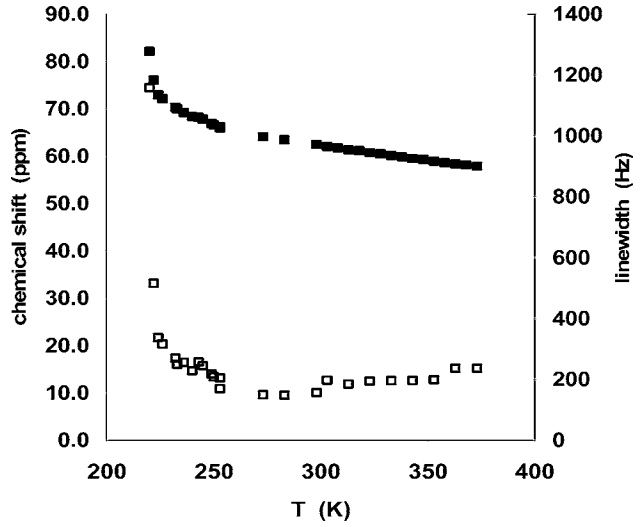

Figure 7. Chemical shift (solid squares) and line width (open squares) of line *a* (open channels) as function of temperature. At $T < 220$ K, line *a* disappears.

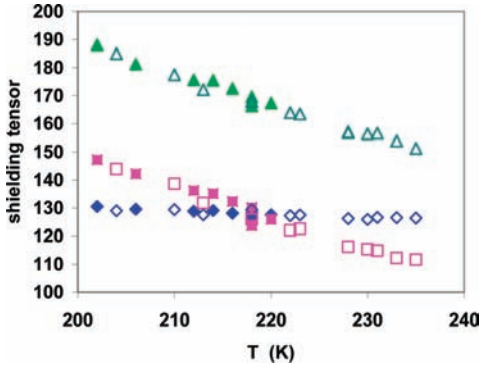

Figure 8. Chemical shift tensor components of line *b* versus temperature: δ_{11} (blue lozenges) along the channel axis, δ_{22} (pink squares) along the minor axis (*d*) of the cross section, and δ_{33} (green triangles) along the major axis (*D*) of the cross section at $P(\mathrm{Xe}) = 1.33$ kPa. Decreasing temperatures, solid symbols; increasing temperatures, open symbols.

K reach a plateau. Surprisingly, in contrast to what happened for CO_2 adsorption in MIL-53, and in the limit of the chosen measurement times, which were supposed to be sufficient for reaching equilibrium, this plateau does not correspond to a total transformation into the *np* form, as shown below by the NMR measurements. This allows us to make two remarks on the effect of decreasing temperatures: (i) the amount of trapped Xe increases (2.7 Xe atoms per unit cell at 220 K) and (ii) fewer Xe atoms are needed to close the channels. Moreover, whatever the adsorbed species, one can note that a threshold amount is necessary in order to observe the shrinkage. For example, for CO_2 adsorption in MIL-53, one molecule per unit cell leaves the structure open, whereas the structure contracts when two molecules are present.

The zone around 220 K is critical. Indeed, the *np* form, which appears at very low pressures (1.2×10^3 Pa), is not the most stable with increasing pressure: above 2.7×10^4 Pa and the kink observed at this pressure, the structure progressively reopens to regenerate the *lp* variety. The same behavior is observed at 195 K, where the initial form is *np*. The reopening begins between 6.7×10^3 and 1.33×10^4 Pa.

From the isotherms, the isosteric heat of adsorption of Xe in both forms can be calculated as a function of the number of

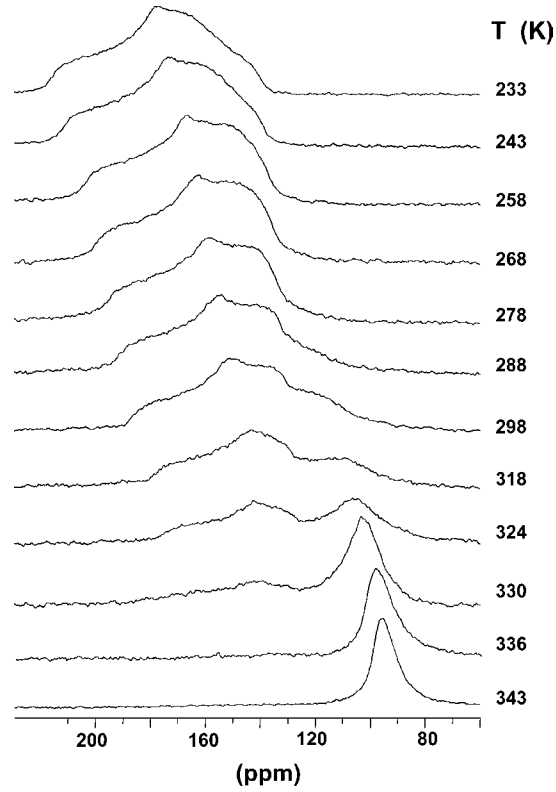

Figure 9. ^{129}Xe NMR spectra versus temperature for $P = 9.6 \times 10^4$ Pa.

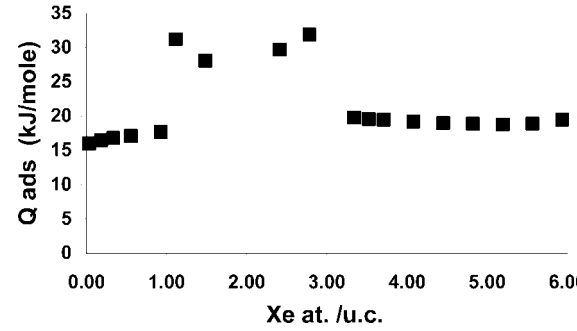

Figure 10. Isosteric heat of adsorption versus Xe loading. For Xe concentration between 1 and 3 Xe atoms/u.c., the porous structure is "closed" (narrow-pore form).

trapped Xe atoms per unit cell (N_{Xe}/u.c.). For the open channels, it can be determined from the isotherms at high temperatures (273, 292, and 333 K) in the domain of low Xe loadings (below 1 Xe atom/u.c.) and from the isotherms at low temperatures (195 and 220 K) in the domain of high Xe loadings (above 3 Xe atoms/u.c.). The results are consistent (Figure 10). The heat of adsorption increases slightly from 16 to 19 kJ/mol for $N_{\mathrm{Xe}} \leq 1$ and is roughly constant (around 19.5 kJ/mol) for $3 \leq N_{\mathrm{Xe}} \leq 6$, values close to those observed with zeolites. In the intermediate concentration range ($1 \leq N_{\mathrm{Xe}} \leq 3$), corresponding to the *np* form, the heat of adsorption reaches ca. 30 kJ/mol. The value obtained for the open form is similar to that measured for zeolites, proving that there is no specific interaction with the organic part of the solid. On the contrary, the high value obtained for the closed form may originate from a specific interaction between Xe and the organics favored by the channel conformation.

Such an interaction could be related to the rotation of the phenyl rings during shrinkage, previously suggested by Brown et al.[31] and recently confirmed through a ^{2}H NMR study.[45] From the study of the adsorption of methane and other light apolar hydrocarbons in MIL-53, it has been suggested that a minimum of ca. 20 kJ/mol in the initial large-pore structure is required to induce the *lp* → *np* structural transition.[19] Thus, the heat of adsorption of methane in MIL-53 (17 kJ/mol) prevents any shrinkage at room temperature.[17] Whereas methane and xenon have similar sizes and heats of adsorption, xenon is able to induce a structural transition of MIL-53. This can be attributed to the high polarizability of the Xe atom.

Variable-Pressure Experiments at 295 K. At this temperature, the only signal visible at pressures below 5.3×10^4 Pa (line *a*) is isotropic and obviously corresponds to the *lp* form, whose accessible diameter is 8.6 Å. The value of the chemical shift δ increases with xenon pressure; its value extrapolated to zero pressure (δ_a) is 60 ppm, in good agreement with that expected for a channel with 8.6 Å diameter using the relationship between chemical shift and pore size established previously.[33] For instance, for the crystallized aluminophosphate AlPO-8, presenting similar one-dimensional channels with pore size of 8.7×7.9 Å^2, $\delta_a = 58$ ppm.[46] This could indicate the absence of any specific interaction of Xe with the organic part of the open skeleton.

The appearance of the anisotropic line *b* around 5.3×10^4 Pa is the signature of the onset of the *np* form, with Xe−surface interactions. At that time, the broadening of line *a* (Figure 3) may indicate a distortion of the open channels induced by the neighboring shrunken ones or a partial exchange between open and closed tunnels (or both). Simultaneously, the slope of the $\delta(P)$ plot increases, likely reflecting a slight decrease of the average pore dimensions of the open channels or, again, a partial dynamic exchange between open and closed channels.

The opposite variations of the intensities of lines *a* (decrease) and *b* (increase) when the pressure is increased (up to $\sim 1.5 \times 10^5$ Pa) evidence the growing importance of the *np* form. At higher pressure (3×10^5 Pa), the intensity of line *a* increases again: the shrunken channels reopen. One can notice that the intensity of line *a* never cancels, which means that, at least in our experimental conditions, the structural transformation is not complete at room temperature. Two interpretations can be provided for this observation: (i) an incomplete transformation of the particles into the closed form or (ii) a collection of either closed- or open-form particles.

In hypothesis (i), the chemical shift hysteresis of line *a* versus Xe loading, while the chemical shift of line *b* is perfectly reversible, could indicate that the pore shrinkage starts at both ends of the channels. In this case, the middle of the channel (in the open form) is separated from the outer gas phase by restrictions (shrunken sections; see scheme in Figure S1, Supporting Information). The Xe loading inside the internal open sections increases with increasing pressure. When the pressure decreases, the shrunken sections prevent the open ones from desorbing. Consequently, the Xe loading, as well as the corresponding chemical shift, remains roughly constant until the pressure is low enough that the shrunken sections reopen. Then, all the adsorbed phase is again in equilibrium with the gas phase, and the chemical shift recovers the value obtained in the experiments performed during Xe adsorption.

In principle, such a mechanism of channel shrinking could be confirmed by a 2D NMR exchange experiment in which only an exchange between shrunken sections (line *b*) and the gas phase can be observed, but it must be rather slow since the diffusion of Xe atoms in the shrunken sections must be slow. No exchange between the open sections (line *a*) and the gas phase would be observed since the open sections are isolated from the gas phase. In addition, an exchange between open and closed sections should occur, supposing a continuous elasticity of the structure despite the large volume variation. Unfortunately, due to the low signal-to-noise ratio, recording a 2D EXSY spectrum is not feasible within a reasonable period of time. Moreover, such an unusual phenomenon would have to be confirmed by a careful *in situ* powder diffraction analysis, which is currently impossible to perform, unfortunately. However, upstream, one can imagine the difficulties for interpreting such a study. The coexistence *in the same grain* of large pores and narrow pores would correspond to a structural disorder at the grain scale, probably characterized by a broadening of the Bragg peaks and/or diffusion peaks.

In hypothesis (ii), the exchange of the Xe atoms between open- and closed-form particles through the interparticle gas phase must be at the origin of the slight decrease of the chemical shift in the region from 1.3 to 0.5×10^5 Pa in the desorption branch. Indeed, in the desorption branch, the proportion of closed form is roughly constant, at maximum value about 72% (vide infra). Therefore, if the chemical shift is an average between those corresponding to the closed- and the open-form particles, it must not vary much since the Xe local concentration is roughly constant (around 2 Xe atoms/u.c.), particularly in the closed form. In this hypothesis, one must consider that line *b* is only slightly modified (in position and shape) by the exchange because the exchange affects only a small fraction of the Xe atoms adsorbed in the closed form, the atoms situated on the border of the channels. In contrast, all the Xe atoms adsorbed in the open particles should exchange owing to the easier diffusion.

Some arguments seem to be in favor of the second hypothesis, i.e., the collection of either closed or open particles. (a) Previous in situ synchrotron diffraction studies[18] proved that, during the drop-by-drop introduction of very dilute solutions of organic molecules in the *np* form of MIL-53(Fe), the part of the *np* structure that comes in contact with the first drops immediately transforms into the *lp* form (the "forceps" effect), which means that, during the introduction, the X-ray powder diffraction (XRPD) patterns of both forms would coexist in these conditions. Nevertheless, this result concerns the *np* → *lp* transition, whereas the reverse transition (*lp* → *np*) is observed in the case of Xe adsorption, and it can be thought that the Xe atoms trapped in the open-form section in the middle of the channels prevent the shrinkage of the channels all along their length. (b) Owing to the large change of the volume during the transition ($\Delta V/V \approx 23\%$ in the case of Xe adsorption, vide infra), it is likely that the limit of elasticity is overcome and that the grains would explode upon the *lp* → *np* transformation, justifying the coexistence of the two forms. (c) The latter hypothesis was recently confirmed by theoretical calculations and simulations which perfectly fit the experimental curves observed for CO_2 adsorption.[16]

Nevertheless, hypothesis (ii) implies an improbable exchange of Xe atoms between open and closed crystals through the gas

(45) Kolokolov, D. I.; Jobic, H.; Stepanov, A. G.; Guillerm, V.; Devic, T.; Serre, C.; Férey, G. *Angew. Chem., Int. Ed.* **2010**, *49*, 4791.
(46) Springuel-Huet, M.-A.; Bonardet, J.-L.; Fraissard, J. *Appl. Magn. Reson.* **1995**, *8*, 427.

phase on the NMR time scale, i.e., a few milliseconds. Assuming a diffusion coefficient of adsorbed Xe on the order of 10^{-9} m^2 s^{-1},[47] the root-mean-square displacement should be about 0.1 μm, which is much smaller than the mean crystal size (on the order of a micrometer).

Synchrotron XRPD experiments could settle the discussion and will be planned as soon as possible.

The isotropic chemical shift of line *b*, extrapolated to zero pressure, is about 136 ppm. Using the relationship between δ and the mean free path of xenon (the difference between the pore diameter and the Xe atom diameter in the case of a cylindrical channel)[48] established with zeolites,[46] this path for a xenon atom would be ca. 1 Å. In the case of cylindrical channels, the average channel diameter would be simply 5.4 Å. In the present case, the large anisotropy of line *b* mainly arises from the elliptical cross section of the channels in the closed form. From NMR data, a rough calculation of the minor (*d*) and major (*D*) axes of the cross section leads to $d = 2.9$ Å and $D = 9.9$ Å (taking 6 Å as the length of the ligand). These values compare fairly with those deduced crystallographically when water is adsorbed, i.e., 2.6 and 13.6 Å, respectively.[16] As the values deduced from NMR experiments concern the region accessible to a Xe atom, it is obvious, from geometrical consideration, that a Xe atom cannot explore the whole free volume of the channels.

Using the correlation between the percentage of breathing of the structure and the molecular size of the guest molecules established by Millange et al.,[18] the unit cell volume should decrease by 23% when xenon is adsorbed (for comparison, it decreases by 32% when water is adsorbed). The closed form of the system Xe@MIL-53 therefore presents pores slightly larger than those of the system H_2O@MIL-53.

One can also estimate the dimensions of the closed-form channels from the maximum number of adsorbed Xe atoms determined from the isotherms. However, it was seen above that the two forms (open and closed) coexist on the plateau of the isotherm, so the value 2.7 Xe atoms/u.c. is not significant. Nevertheless, it can be calculated (vide infra).

The components of the chemical shift tensor of line *b* have been assigned. The contribution to the shielding in a given direction is determined by the electron density around the nucleus in the perpendicular plane.[49] Consequently, the constant component, δ_{11}, is the one along the channel axis because the perpendicular plane is the channel cross section and the interaction of Xe atoms with the solid surface should not depend much on the Xe concentration. The most deshielded component (higher chemical shift), δ_{33}, should be along the *D* direction, perpendicular to both the channel axis (along which the Xe−Xe interaction occurs essentially) and the minor *d* axis of the cross section (along which the Xe−surface interaction is the most important). Finally, δ_{22} is the component along the minor axis.

It has been shown that, for Xe adsorbed in a medium-bore pipe, the shielding tensor component parallel to the pipe axis ($\sigma_{\parallel}$) is the most deshielded at the zero loading limit.[49] When the Xe loading increases, $\sigma_{\parallel}$ remains constant while the two perpendicular components ($\sigma_{\perp,1}$ and $\sigma_{\perp,2}$) increase and become larger than $\sigma_{\parallel}$ at full loading. In the case of the Xe@MIL-53 system, when the Xe loading is high enough to make the open channels shrink, the Xe loading inside the closed channels is already rather high, and we are in an intermediate case where $\sigma_{\parallel} \approx \sigma_{\perp,1}$ and $\sigma_{\perp,2} > \sigma_{\parallel}$ in the first spectra.

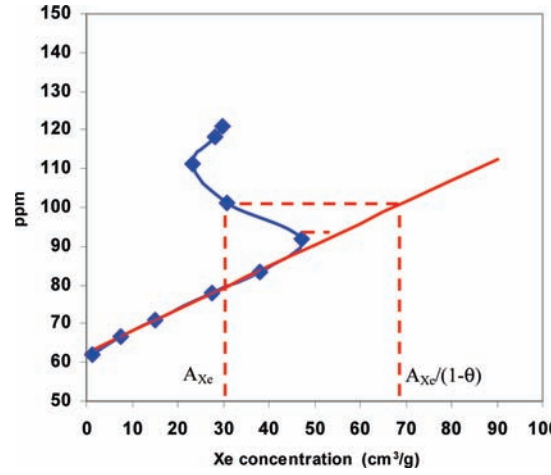

Figure 11. Chemical shift (blue symbols) of line *a* (open channels) versus the amount of Xe adsorbed in the open channels. Solid red line is the linear transformation of the linear part of the blue curve.

It is obvious from the NMR spectra that the structure does not shrink completely, since line *a* never disappears (Figure 3). The intensity of the NMR lines is proportional to the number of Xe nuclei adsorbed in the corresponding environments, which is proportional itself to the local Xe concentration, N_{Xe} (Xe atoms/u.c.), and to the number of unit cells of a given type (open or closed). Therefore, the relative quantities of open and closed channels can be deduced. The local concentration is not known, but the chemical shift is proportional to it. Let us consider the line *a* corresponding to the open form and the plot of its chemical shift variation as a function of the amount of xenon adsorbed in open channels, A_{Xe}, obtained from the adsorption isotherm and the intensity of line *a* (Figure 11). This quantity has to be referred to the amount of sample and can be expressed as the volume (at standard temperature and pressure) of xenon gas adsorbed per gram of solid, for example. The first part of the curve is linear. It corresponds to the increase of Xe−Xe interactions inside the open channels, and the slope of the curve is proportional to the local concentration, N_{Xe}. The chemical shift can be written as

$$\delta - 60 = kN_{Xe}$$

where 60 is the value of the intercept. Since $A_{Xe} = N_{Xe}n_{u.c./g}$, therefore,

$$\delta - 60 = \frac{k}{n_{u.c./g}}A_{Xe}$$

where $n_{u.c./g}$ is the number of unit cells (open form) per gram. Before the transition occurs, all the unit cells are in open form. The slope of the first part is $k/n_{u.c./g}$.

When the pore structure begins to shrink (above $P = 4 \times 10^4$ Pa or above $A_{Xe} = 40$ cm^3/g), the number of open-form unit cells diminishes from a fraction θ (corresponding to the fraction of closed channels formed) and the expression of the chemical shift becomes

$$\delta - 60 = \frac{k}{n_{u.c./g}(1-\theta)}A_{Xe}$$

(47) Heink, W.; Kärger, J.; Pfeifer, H.; Stallmach, F. *J. Am. Chem. Soc.* **1990**, *112*, 2175.
(48) Springuel-Huet, M.-A.; Ph.D. thesis, Université P. et M. Curie, Paris, France, 1988.
(49) Jameson, C. J.; de Dios, A. C. *J. Chem. Phys.* **2002**, *1169*, 3805.

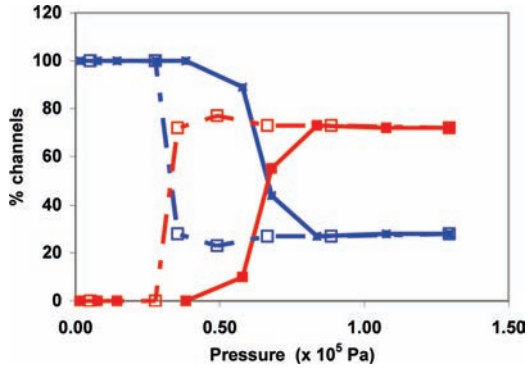

Figure 12. Percentage of open (blue) and closed (red) channels as a function of pressure at Xe adsorption (solid symbols) and desorption (open symbols).

The slope is evidently higher and the values of the chemical shift are above the straight line of slope $k/n_{u.c./g}$. Since A_{Xe} decreases, because a fraction of the open channels disappears, the curve shows a "snake" shape. If we project the chemical shift points onto the straight line, the corresponding abcissa is therefore $A_{Xe}/(1-\theta)$, and we can determine θ, the fraction of open channels transformed into closed channels.

The percentage of open $(1-\theta)$ and closed (θ) channels can therefore be determined as a function of Xe pressure for adsorption and desorption at room temperature (Figure 12). One can see that, during adsorption, the channels begin to shrink for $P > 4 \times 10^4$ Pa, and the process stops at $P \approx 8 \times 10^4$ Pa, when 72% of the channels have shrunk. This percentage remains roughly constant for pressures up to 1.2×10^5 Pa. Since the spectrum recorded for $P \approx 3 \times 10^5$ Pa shows that the intensity of line *a* has largely increased compared to that at $P \approx 1.2 \times 10^5$ Pa, it can be concluded that some of the closed channels have reopened, but we cannot calculate the proportion because the adsorption isotherm is not known at this pressure.

It is clear from the spectra that, during desorption, the closed channels do not reopen before the Xe pressure becomes lower than 3.5×10^4 Pa. At $P \approx 2.8 \times 10^4$ Pa, all the channels are in open form again.

Knowing the percentage of each type of channels as a function of pressure, we can plot the chemical shift variation versus the genuine local concentration (Figure 13). It can be observed that the chemical shift variation of line *a* is practically the same during adsorption and desorption, proving that the size and the shape of the open channels are not modified when closed channels are formed. The small hysteresis observed above 6.7×10^4 Pa might correspond to a slight decrease of the dimensions of the open channels due to the deformation of the surroundings or, simply, might be due to uncertainty, especially in the signal decomposition.

It can be seen that the local concentration in the closed channels does not vary very much around 1.8−2 Xe atoms per unit cell, whatever the pressure. Moreover, knowing the percentage of each type of channel and the local concentration of Xe determined from the chemical shift, we can determine the adsorption isotherms of Xe in each type of channel and calculate the total amount of Xe adsorbed (Figure 14). It compares well with the experimental adsorption isotherm, especially at pressures above 6.7×10^4 Pa. At $P = 5.8 \times 10^4$ Pa, the intensity of line *b* is very weak, and the relative error may be important, explaining the discrepancy between the two curves in this region.

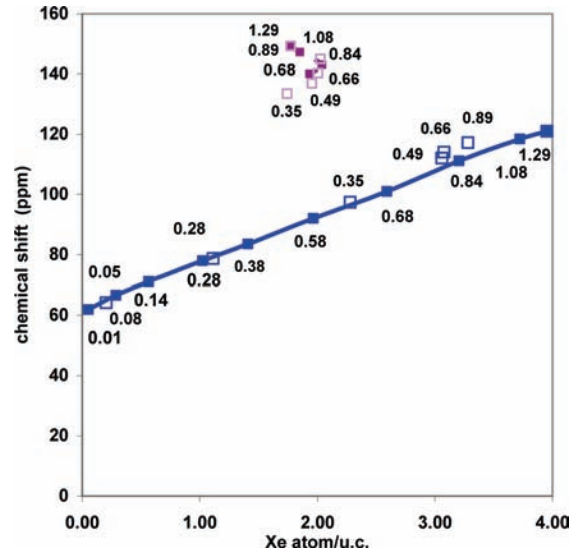

Figure 13. Chemical shift of Xe adsorbed in open (blue) and closed (red) channels as functions of the local concentration at Xe adsorption (solid symbols) and desorption (open symbols). Numbers on the curves correspond to the Xe pressures in Pa ($\times 10^5$).

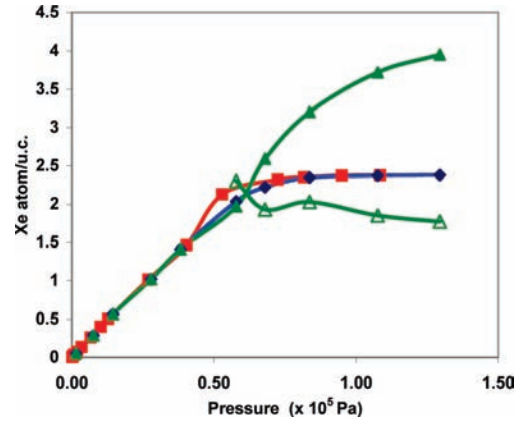

Figure 14. Xe adsorption isotherms measured volumetrically (red) and calculated from NMR data for each type of channel (green; solid symbols, open channels; open symbols, closed channels), and for the whole sample (blue). $T = 293$ K.

Variable-Temperature Experiments. At low pressure, the sudden change in the spectra around 221 K shows that the structure switches from the *lp* (above 221 K) to the *np* form (below 221 K). The two forms coexist within only a short temperature range (5−6 K). Before the phase transition, both the chemical shift and the width of line *a* drastically increase. This corresponds to a large increase in the amount of adsorbed Xe in the channels and to the beginning of the structure deformation, which leads to a heterogeneous distribution of channel dimensions. The low temperature and the high amount of adsorbed Xe (made possible by the large quantity of gaseous Xe available in the volume of the hyperpolarization device, about 0.25 L) can induce the complete transformation of the whole solid.

The disappearance of the signal for temperatures below 200 K is due to the decrease of the mobility of the Xe atoms inside the closed channels; the hyperpolarized xenon is not able to penetrate the channels within the repetition time (1 s) of the pulse sequence.

When the temperature is increased from 200 K, the reverse *np* → *lp* transformation occurs at temperatures higher than 221

K. Line *b* is still observed up to 245 K, and the chemical shift tensor components have been determined for temperatures up to 235 K. The δ_{22} and δ_{33} components decrease when temperature increases, and above 220 K, the δ_{22} component becomes smaller than the constant component, δ_{11}, approaching the situation that must be observed at zero loading, where the constant component must be the highest.[49] In the case of MIL-53 material, the closed channels do not exist at very low loading. At room temperature, when the closed channels are formed, the Xe concentration is high enough to lead to δ_{22} and $\delta_{33} \geq \delta_{11}$, which is also the case, at low pressure (1.3 kPa), when the closed channels are formed at 221 K. Owing to the temperature hysteresis, with increasing temperature, the channels remain closed above 221 K and therefore at lower loading, allowing δ_{11} to be greater than one of the two other components.

The complete transformation is not observed in the experiment performed with thermally polarized Xe at $P = 9.6 \times 10^4$ Pa (measured at room temperature) in a sample tube of about 3 cm^3 because the quantity of gaseous Xe is negligible compared to the quantity adsorbed. Therefore, the amount of adsorbed Xe remains practically constant when temperature decreases.

On the other hand, increasing the temperature favors the open form, and the intensity of line *a* increases. Above 333 K, the whole solid adopts the open form, despite the high pressure in the sample tube (estimated from the isotherms to be 2.7×10^5 Pa), corresponding to a Xe loading of 2.9 atoms per unit cell. At this temperature, even if the loading is larger than 2 Xe atoms/u.c., which is necessary to make the framework shrink at lower temperatures, all the channels remain open. This is consistent with the Xe@MIL-53 phase diagram recently obtained.[40]

V. Conclusion

In this paper, we have reported that xenon is able to induce a structural transformation of MIL-53 materials from a large-pore form to a narrow-pore form. Xenon adsorption isotherms and ^{129}Xe NMR spectroscopy have been used to monitor the impact of xenon pressure and temperature on the structural transition. This study reveals a more detailed description of the already-known flexibility of this MOF material, where the framework can adapt the dimensions of the pores in order to optimize the interactions with the adsorbate. Xenon chemical shift is known to be extremely sensitive to its environment; in particular, it is able to discriminate between pores with different pore sizes. The relevance of the reported results lies in the use of the chemical shift as a measurement of the local xenon amount and, consequently, in the first spectroscopic quantification of the extent of transformation from large to narrow pores in MIL-53 materials. We have demonstrated that this transformation is not complete at room temperature. However, a total transformation can be achieved by decreasing the temperature. In addition, the hysteresis of the chemical shift variation versus xenon pressure observed for the signal corresponding to the large-pore form can be explained by an exchange of the Xe atoms, through the gas phase, between open- and closed-form particles or by a shrinkage of the one-dimensional pores at both ends.

Supporting Information Available: Scheme of the channel shrinking, magic angle spinning spectra, and spectrum decomposition. This material is available free of charge via the Internet at http://pubs.acs.org.

JA103105Y